IOP Conf. Series: Materials Science and Engineering **730** (2020) 012019 doi:10.1088/1757-899X/730/1/012019

Research on Damping Characteristics of Photo-controlled Electrorheological Damper

Xiang Liu, Yusong Chen and Xinjie Wang

School of Mechanical Engineering, Nanjing University of Science and Technology, Nanjing, China.
Email: xjwang@njust.edu.cn

Abstract. Firstly, the expression of PLZT ceramic driving voltage is obtained with external load. Furthermore, the hydrodynamic modelling of the electrorheological fluid in the circular damping channel is carried out, and the relationship between the pressure difference between the two ends of the damping channel and the PLZT ceramic driving voltage is derived, and the hydrodynamic simulation of the electrorheological fluid in the circular damping channel was carried out in the fluid simulation software Fluent. The simulation result shows the correctness of the mathematic model and the feasibility of photo-controlled electrorheological damper.

1. Introduction

Electrorheological fluid is a kind of intelligent soft material with potential application. It has the electrorheological effect, that is, it exhibits the characteristics of Newtonian fluid when no electric field is applied. When the electric field is applied, its viscosity changes and it changes from liquid to solid. The change will quickly return to a liquid form after the electric field is removed. Electrorheological fluids are widely used in dampers, shock absorbers, and automotive suspension systems. However, the conventional ER damper requires an external boost circuit to provide a high-value electric field, which causes the entire damper device to have a complicated structure, be susceptible to electromagnetic interference, and not easily miniaturized.

Another smart material is called yttrium-modified zirconate titanate ceramic (PLZT), which generates anomalous photovoltaic effects under the excitation of a specific wavelength of ultraviolet light source, and produces a high-value photo-generated voltage of several kV/cm in the polarization direction. Therefore, combining the above two smart materials, the high-value photo-generated voltage generated by the PLZT ceramic under the high-energy ultraviolet light source is applied to the electrorheological damping device, such that the electrorheological damping device has a simple structure, no electromagnetic interference, and can work in a vacuum environment.

The anomalous photovoltaic effect of PLZT ceramics was first discovered by the phenomenon that the photo-generated voltage in BaTiO3 observed by Volk[1] et al. in 1973, which is much larger than the solid forbidden band width. In 1975, Brody[2] pointed out that the photo-generated voltage of PLZT ceramics depends on factors such as material, grain size, and material bulk temperature. Later scholars tried to explain the mechanism of this phenomenon with an electrical model. In 1983, Brody[3] used the RC equivalent electrical model to describe this phenomenon. In 1988, Poosanaas[4] studied the anomalous photovoltaic effect under different components, and pointed out that the maximum photo-generated current and photo-generated voltage appeared under the components of 4/48/52 and 5/54/46, respectively. Sun and Tong[5] et al. studied the effect of temperature on the photo-induced voltage of PLZT ceramics and proposed a corresponding equation. Using the

anomalous photovoltaic effect of PLZT ceramics, Morikawa[6] proposed a new type of photoelectric motor.

In 1949, Winslow[7] prepared an electrorheological fluid by dispersing flour and lime in silicone oil and found the electrorheological effect. Later scholars proposed many related models. In 1983, Stangroom[8] and others proposed a water bridge model, and the flow of electrorheological fluid must overcome the "water bridge force" between the particles. Klass[9] proposed an electric double layer model, which better explains the effects of external temperature and voltage and the concentration of electrorheological fluid on the electrorheological effect. Davis[10] and Atten[11] proposed a conductivity model for the anhydrous electrorheological fluid. The model considers that the main cause of the electrorheological effect is the ratio of the conductivity of the suspended particles to the base fluid. The electrorheological fluid has the advantage of fast response speed, convenient regulation and easy control, so it is widely used in engineering fields such as damping systems, vibration and noise reduction systems, brake systems, electromechanical coupling control and liquid valves.

In this paper, the expression of PLZT ceramic driving voltage is obtained with external load. Secondly, the hydrodynamic modeling of the electrorheological fluid in the circular damping channel is carried out, and the relationship between the pressure difference between the two ends of the damping channel and the PLZT ceramic driving voltage is derived, and the hydrodynamic simulation of the electrorheological fluid in the circular damping channel was carried out in the fluid simulation software Fluent. Finally, the comparison between theoretical and simulation result is made to verify the correctness of the mathematical model.

2. Mathematical Modelling of Photo-controlled Electrorheological Damping

2.1. Photo-controlled Electrorheological Damping Device Structrue

The schematic diagram of the structure of the photo-controlled electrorheological damping device is shown in figure 1.

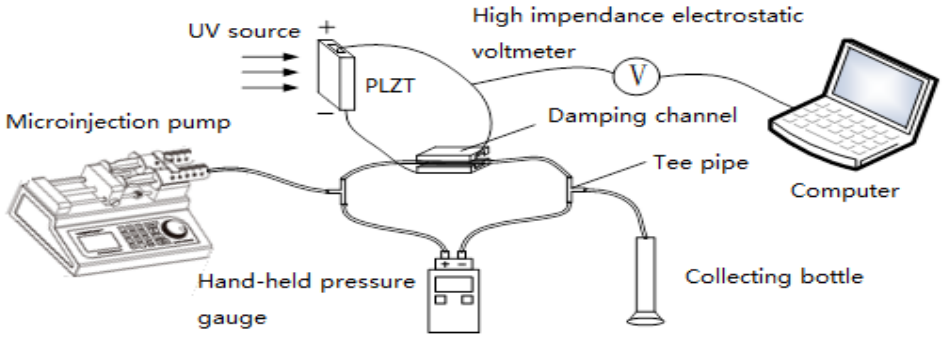

Figure 1. Schematic diagram of experimental platform for light-controlled electrorheological damping device.

When PLZT ceramic is irradiated vertically by the ultraviolet light with a wavelength near 365 nm, the photo-generated carriers flow along the polarized direction, so that the positive electrode and the negative electrode of the PLZT ceramic collect the positive and negative charges respectively to generate a high photovoltaic voltage of several kV/cm. The silver wire is used to connect the electrodes of the PLZT ceramic to the two pieces of copper foil which are attached to the top and the bottom side of the damping channel respectively with the insulating adhesive. Therefore, the electric field required for the electrorheological fluid in the damping channel is provided.

2.2. Mathematical Modelling of Photo-generated Driving Voltage

When the two ends of the PLZT ceramic are respectively connected to the parallel copper foil plate load through the silver wire, the equivalent electrical model of the external load is shown in figure 2.

R_d and C_d are the resistance and capacitance of the parallel plate generated by two parallel copper foils respectively.

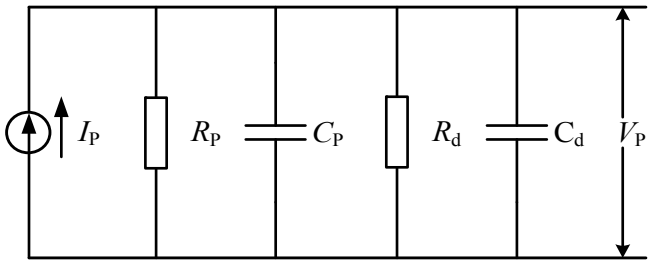

Figure 2. Equivalent electrical model of PLZT ceramics with external load.

According to the new equivalent circuit model above, the driving voltage produced by PLZT ceramic for electrostatic parallel plate is:

$$V_P = I_P \frac{R_P \cdot R_d}{R_P + R_d}(1 - e^{-\frac{t}{\tau}}) = V_s(1 - e^{-\frac{t}{\tau}}) \tag{1}$$

where τ is the time constant, the expression is:

$$\tau' = \frac{R_P \cdot R_d}{R_P + R_d}(C_P + C_d) \tag{2}$$

2.3. Hydrodynamic Model of Electrorheological Fluid in Damping Channel

When the electrorheological fluid flows in a steady state in the circular damper channel, the force is shown in figure 3.

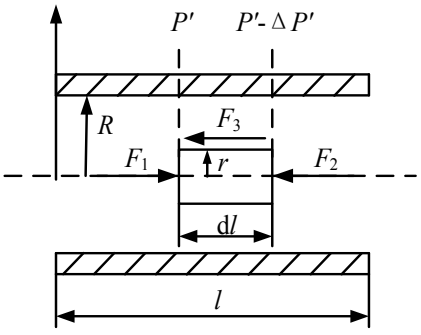

Figure 3. The force of electrorheological fluid in a circular damping channel.

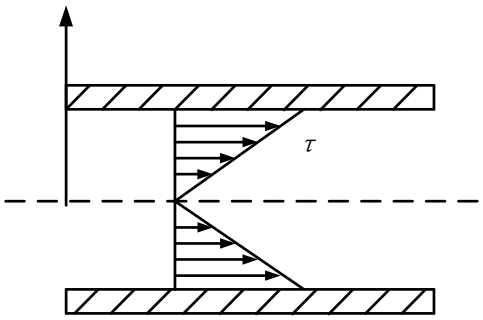

Figure 4. Electrorheological fluid shear stress distribution map.

From the liquid balance equation: $\Sigma F=F_1+F_2+F_3=0$, we can get:

$$\pi r^2 P' - \pi r^2 (P' - \Delta P') - 2\pi r\tau(r)\mathrm{d}l = 0 \tag{3}$$

Simplify formula (4):

$$\tau(r) = \frac{r\Delta P'}{2\mathrm{d}l} = \frac{r\Delta P}{2L} \tag{4}$$

Where ΔP is the pressure difference across the circular damper channel; L is the length of the circular damper channel.

It can be seen from equation (4) that the electrorheological fluid is proportional to the radius in both the Newtonian fluid and the Bingham fluid in the circular damping channel, as shown in figure 4.

2.3.1. Dynamic Model of Electrorheological Fluid without Electric Field. When there is no electric field, the electrorheological fluid exhibits the characteristics of Newtonian fluid. In a circular damper channel, the constitutive model is:

$$\tau(r) = -\eta \frac{\mathrm{d}u(r)}{\mathrm{d}r} \tag{5}$$

Where τ(r) is the shear stress of the electrorheological fluid; du(r)/dr is the shear rate; u(r) is the horizontal flow velocity of the electrorheological fluid; η is the plastic viscosity or dynamic viscosity independent of the electric field strength.

Bringing equation (5) into equation (4) and integrating it. Note that u(r)|r=R=0, from which the Poiseuille equation for the radial flow velocity distribution of the Electrorheological fluid along the damper channel is obtained:

$$u(r)=\frac{\Delta P}{4\eta L}(R^2 - r^2) \tag{6}$$

From the flow formula of the liquid ,we can obtain that:

$$Q=2\pi\int_0^R u(r)r\mathrm{d}r=\frac{\pi R^4}{8\eta L}\Delta P \tag{7}$$

When there is no electric field, the relationship between the pressure drop and the flow when the electrorheological fluid exhibits Newtonian fluid properties is:

$$\Delta P=(P_{in} - P_{out})=\frac{8\eta L}{\pi R^4}Q \tag{8}$$

2.3.2. Dynamic Model of Electrorheological Fluid when loading Electric Field. When the photo-generated voltage generated by the PLZT ceramic excited by the high-energy ultraviolet light source is applied to the copper foil plate on the upper and lower sides of the damping channel, the electrorheological fluid exhibits Bingham fluid characteristics under the action of the electric field. The velocity distribution of Bingham fluid in a circular damper channel is shown in figure 5.

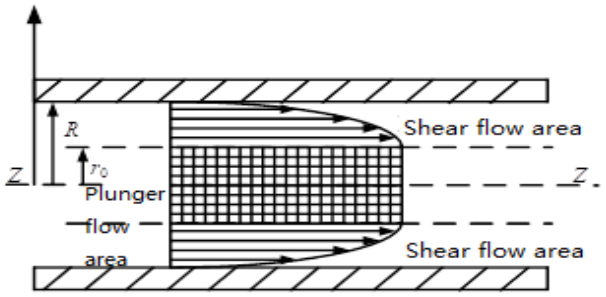

Figure 5. Velocity distribution of Bingham fluid in a circular damping channel

As can be seen from Figure 4, the flow rate of the electrorheological fluid is divided into two parts, when $r < r_0$, it is the plunger flow area; when $r > r_0$, it is the shear flow area. Where r_0 is the radius of the "cylinder plug".

Within the region I ($r_0 < r < R$):

$$\tau(r)=\tau_y(E)-\eta\frac{\mathrm{d}u(r)}{\mathrm{d}r} \tag{9}$$

Note that u(r)|r=R=0, you can get:

$$u(r)=\frac{\Delta P}{4\eta L}(R^2-r^2)-\frac{\tau_y}{\eta}(R-r) \tag{10}$$

In the region II (0<r< r_0), since du(r)/dr=0, there is $\tau(r_0)=\tau_y$, and substituting into the equation (4) can obtain the "cylinder plug" radius r_0

$$r_0=\frac{2\tau_y L}{\Delta P} \tag{11}$$

Since u(r)= u(r_0)=C, there are:

$$u(r)=\frac{\Delta P}{4\eta L}(R^2-r_0^2)-\frac{\tau_y}{\eta}(R-r_0) \tag{12}$$

According to the flow formula of the liquid and integrate it, you can get:

$$\Delta P^4-(\frac{8\tau_y L}{3R}+\frac{8\eta L}{\pi R^4}Q)\Delta P^3+\frac{1}{3}(\frac{2\tau_y L}{R})^4=0 \tag{13}$$

Equation (13) can be simplified when the flow rate Q is large:

$$\Delta P=(P_{in}-P_{out})=\frac{8\eta L}{\pi R^4}Q+\frac{8\tau_y L}{3R} \tag{14}$$

The relationship between the dynamic yield stress τ_y and the electric field strength E can be expressed as:

$$\tau_y=kE^{\alpha} \tag{15}$$

Therefore, when the high-value electric field generated by the PLZT ceramic excited by the high-energy ultraviolet light source is used as the driving electric field of the electrorheological fluid, the expression of the pressure difference ΔP at both ends of the circular damping channel is obtained:

$$\Delta P=\frac{8\eta L}{\pi R^4}Q+\frac{8L}{3R}k\left(\frac{V_{\mathrm{mod}}}{d}\right)^{\alpha}=\frac{8\eta L}{\pi R^4}Q+\frac{8L}{3R}k\left(\beta I_{\mathrm{P}}(\frac{R_{\mathrm{P}}R_{\mathrm{d}}}{R_{\mathrm{P}}+R_{\mathrm{d}}})(1-e^{-\frac{t}{(C_{\mathrm{P}}+C_{\mathrm{d}})R_{\mathrm{P}}R_{\mathrm{d}}/(R_{\mathrm{P}}+R_{\mathrm{d}})}})/d\right)^{\alpha} \tag{16}$$

2.4. Influence of Light Intensity I on the Pressure difference across the Damping Channel

The relationship between the pressure difference across the damper channel and the light intensity I can be obtained by the relationship between the driving voltage V_{mod} and the light intensity I:

$$\Delta P=\frac{8\eta L}{\pi R^4}Q+\frac{8L}{3R}k\left(\beta A_{\mathrm{cur}}A_{\mathrm{r}}I^{\alpha_{\mathrm{cur}}-\alpha_{\mathrm{r}}}\frac{R_{\mathrm{d}}}{A_{\mathrm{r}}I^{-\alpha_{\mathrm{r}}}+R_{\mathrm{d}}}(1-e^{-\frac{t}{\tau'}})/d\right)^{\alpha} \tag{17}$$

The fitting values of the PLZT ceramic photo-generated voltage characteristics index obtained through experiments are shown in table 1:

Table 1. PLZT ceramic photo-generated voltage characteristics index fitting value.

Photocurrent coefficient A_{cur}	Photo-resistance coefficient A_r	Photocurrent varies with light intensity α_{cur}	Photo-resistance varies with light intensity α_r
7.368×10^{-14}	1.052×10^{16}	1.512	1.293

Considering the damping channel upper and lower copper foil plate geometry is 20mm (l) × 5mm (w), the gap(d) is 3mm, according to the parameter fitting value in table 1, the variation curve of the pressure difference ΔP saturation value across the corresponding damping channel when the light intensity is gradually increased from 0 to 400 mW/cm^2 is shown in figure 6:

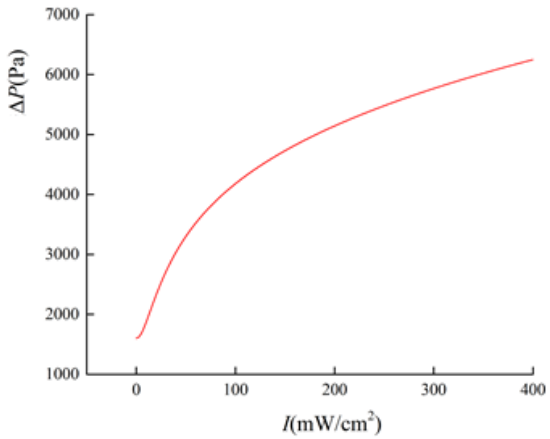

Figure 6. Curve of pressure difference across the damper channel as a function of light intensity

It can be seen from figure 6 that as the light intensity I gradually increases from 0 to 400 mW/cm^2, the pressure difference ΔP across the damping channel gradually increases, and when the light intensity is 0, the pressure difference is not zero since the electrorheological fluid still has viscosity at this time. When the light intensity changes in the range of 0-100 mW/cm^2, the pressure difference ΔP grows faster, and then the pressure difference increases gradually with the increase of light intensity, which is caused by the characteristics of PLZT ceramics: the PLZT ceramic driving voltage saturation value does not increase endlessly with the increase of light intensity.

3. Simulation of Light-controlled Pressure Difference Response Characteristics based on Fluent

Firstly, the model is established and meshed for the circular damping channel. The two ends of the damping channel are defined as velocity input and pressure output respectively. Secondly, the appropriate fluid model and solver are selected in Fluent. Finally, the calculation results in Fluent are imported. In the processing software Tecplot, the pressure and velocity clouds can be obtained, as well as the pressure difference ΔP across the damping channel, as shown in figure 7.

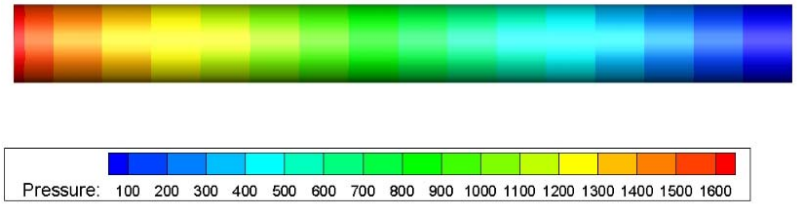

Figure 7. Damping channel pressure cloud map ($\tau_y = 0$)

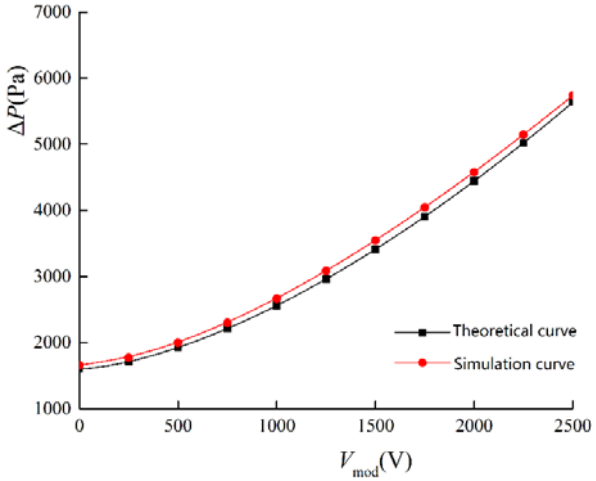

Figure 8. Curve of pressure difference across the damping channel as a function of driving voltage

According to the different driving voltage V_{mod} of PLZT ceramics, the dynamic shear yield stress τ_y of the electrorheological fluid can be calculated, and the corresponding dynamic shear yield stress can be set in the material property setting interface. After the flow field is initialized, the simulation can be obtained. The comparison curve between the pressure difference simulation results and the theoretical results is shown in figure 8.

It can be seen from figure 8 that the theoretical curve and the simulation curve are almost coincident, and the error between the theoretical pressure difference and the simulated pressure difference is within 5%, which proves the correctness of the theoretical mathematical model.

4. Conclusions

In this paper, a new way of photo-controlled electrorheological damper based on PLZT ceramics is proposed. By modifying the expression of the static voltage of PLZT ceramic without load, the equivalent electrical model of PLZT ceramic with external load of the electrorheological channel is obtained. The hydrodynamic modelling of the electrorheological fluid in the circular damping channel is deduced, and the relationship between the pressure difference between the two ends of the damping channel and the PLZT ceramic driving voltage is derived.

The pressure difference ΔP across the damping channel increases with the increase of light intensity under the premise of other conditions remain unchanged. The correctness of the mathematic model is verified by comparing the theoretical result and the simulation result which is obtained through Fluent.

5. Acknowledgements

The authors gratefully acknowledge the funding support from the National Natural Science Foundation of China (No.51675282)

6. References

[1] Volk T R, Grekov A A, Kosonogov N A, et al. (1973). Influence of illumination on the domain structure and Curie temperature of BaTiO3. *Sov. Phys.-Solid State*, **14**, 2740-2743.
[2] Brody P S. (1975). High voltage photovoltaic effect in barium titanate and lead titanate-lead zirconate ceramics. *Journal of Solid State Chemistry*, **12(3)**, 193-200.
[3] Brody P S. (1983). Optomechanical bimorph actuator. *Ferroelectrics*, **50(1)**, 27-32.
[4] Poosanaas P, Uchino K. (1999). Photostrictive effect in lanthanum-modified lead zirconate titanate ceramics near the morphotropic phase boundary. *Materials Chemistry & Physics*, **61(1)**, 36-41.
[5] Sun D, Tong L. (2007). Modeling of wireless remote shape control for beams using nonlinear photostrictive actuators. *International Journal of Solids and Structures*, **44(2)**, 672-684.

[6] Morikawa Y, Ichiki M, Nakada T. (2006). Electrostatic Optical Motor Using PLZT Elements. *The Japan Society of Mechanical Engineers*, **72(718)**, 1807-1811.
[7] Winslow W M. (1949). Induced Fibration of Suspensions. *Journal of Applied Physics*, **20(12)**, 1137-1140.
[8] Stangroom J E. (1983). Electrorheological Fluids. *Physical Technology,* 1983, **14(6)**, 290–296.
[9] Klass D L, Martinek T W. (1967). Electroviscous Fluids. I. Rheological Properties. *Journal of Applied Physics*, **38(1)**, 67-74.
[10] Davis L C. (1992). Ground state of an electrorheological fluid. *Physical Review A*, **46(2)**, 719-721.
[11] Atten P. (1994). Conduction model of the electrorheological effect. *International Journal of Modern Physics B*, **8(20-21)**, 2731-2745.